ELSEVIER

Nuclear Instruments and Methods in Physics Research A 440 (2000) 5–16

NUCLEAR INSTRUMENTS & METHODS IN PHYSICS RESEARCH Section A

www.elsevier.nl/locate/nima

Charge collection efficiency of irradiated silicon detector operated at cryogenic temperatures

RD39 Collaboration

K. Borer[a,*], S. Janos[a], V.G. Palmieri[a,1,2], B. Dezillie[b,3], Z. Li[b,3], P. Collins[c], T.O. Niinikoski[c], C. Lourenço[c], P. Sonderegger[c], E. Borchi[d], M. Bruzzi[d], S. Pirollo[d], V. Granata[e,4], S. Pagano[e], S. Chapuy[f], Z. Dimcovski[f], E. Grigoriev[f], W. Bell[g], S.R.H. Devine[g], V. O'Shea[g], K. Smith[g], P. Berglund[h], W. de Boer[i], F. Hauler[i], S. Heising[i], L. Jungermann[i], L. Casagrande[j], V. Cindro[k], M. Mikuž[k], M. Zavartanik[k], C. da Viá[1,4], A. Esposito[l], I. Konorov[l], S. Paul[l], L. Schmitt[l], S. Buontempo[m], N. D'Ambrosio[m], S. Pagano[m], G. Ruggiero[m], V. Eremin[n], E. Verbitskaya[n]

[a]*Laboratorium für Hochenergiephysik der Universität Bern, Sidlerstarsse 5, CH-3012 Bern, Switzerland*
[b]*Brookhaven National Laboratory, Upton, NY 11973-5000, USA*
[c]*CERN, CH-1211 Geneva, Switzerland*
[d]*Dipartimento di Energitica, Università di Firenze, I-50139 Firenze, Italy*
[e]*Istituto di Cibernetica del CNR, I-80072 Arco Felice, Italy*
[f]*Department de Radiologie, University de Geneve, CH-1211 Geneva, Switzerland*
[g]*Department of Physics and Astronomy, University of Glasgow, Glasgow G12 8QQ, UK*
[h]*Low Temperature Laboratory, Helsinki University of Technology, FI-02150 Espoo, Finland*
[i]*IEKP University of Karlsruhe, D-76128 Karlsruhe, Germany*
[j]*LIP, av. E. Garcia, P-1000 Lisbon, Portugal*
[k]*Jožef Stefan Institute, Exp. Particle Physics Dep., PO Box 3000, 1001 Ljubljana, Slovenia*
[l]*Physik Department E18, Technische Universität München, D-85748 Garching, Germany*
[m]*Universitá Frederico II di Napoli, Dipartimento di Fisica and INFN, Napoli, Italy*
[n]*Ioffe Physico-Technical Institute, Russian Academy of Sciences, St. Petersburg 194021, Russia*

Received 22 July 1999; accepted 2 August 1999

Abstract

The charge collection efficiency (CCE) of heavily irradiated silicon diode detectors was investigated at temperatures between 77 and 200 K. The CCE was found to depend on the radiation dose, bias voltage value and history, temperature, and bias current generated by light. The detector irradiated to the highest fluence 2×10^{15} n/cm^2 yields a MIP signal of at least 15000 e$^-$ both at 250 V forward bias voltage, and at 250 V reverse bias voltage in the presence of a light-generated current. The "Lazarus effect" was thus shown to extend to fluences at least ten times higher than was previously studied.

* Corresponding author. Tel.: + 41-22-767-6079; fax: + 41-22-785-0672.

E-mail addresses: vittorio.palmieri@cern.ch (V.G. Palmieri), tapio.niinikoski@cern.ch (T.O. Niinikoski)

[1] Now at CERN.

[2] Correspondence may also be addressed to V.G. Palmieri.

[3] This investigation was done as a part of work established by the U.S. Department of Energy: Contract No. DE-AC02-98CH10886.

[4] Now at Brunel University.

0168-9002/00/$ - see front matter
PII: S0168-9002(99)00799-8

1. Introduction

The so-called Lazarus effect, phenomenologically described as the recovery of the Charge Collection Efficiency (CCE) of heavily irradiated silicon detectors when cooled to cryogenic temperatures, was observed for the first time in 1998 [1] and has been studied by the CERN RD39 collaboration [2]. The present work extends the study of the CCE over more than an order of magnitude in fluence, covering the range equivalent to 1×10^{14}–$2\times10^{15}\,\mathrm{cm}^{-2}$ of 1 MeV neutrons.[5] The normalization to 1 MeV neutrons relies on calculation [3] using the spectrum measured with activation of foils and the published damage factors; this agrees well with the method based on the measurement of the leakage current [4] and yields a damage constant equal to 0.9 for the reactor neutrons with energy above 100 keV relative to the monochromatic 1 MeV neutrons.

In this paper we report results on diode detectors irradiated to fluences above the bulk-type inversion threshold. The samples and the apparatus are described in Section 2, and the I–V characteristics of the devices after annealing are given in Section 3. The temperature, voltage and time dependences of the CCE were measured down to 77 K and are discussed in Section 4. For three samples in which the forward current was low enough to allow a measurement, the CCE at forward bias voltage is also reported in Section 5, together with the study of the CCE under illumination by light of different wavelengths. The influence of annealing was also determined and is shown in Section 5. The results are finally discussed in Section 6.

In the accompanying paper [5] results are presented for an irradiated double-sided silicon microstrip detector operated at low temperatures. The data yield results on the cluster sizes on both sides, and enable conclusions to be drawn on the mechanisms of the changes of the CCE. These extend and strengthen the conclusions reached in this paper.

[5] The fluence values given in this paper are always normalized to these units, denoted as n/cm^2.

2. Samples and experimental set-up

The devices investigated are DC-coupled Al/p$^+$/n/n$^+$/Al implanted silicon detectors processed at BNL (Brookhaven National Laboratory, USA) on n-type 4″ wafers of various thicknesses. The n$^+$ implant covers homogeneously the back side of the wafer from which the diodes are fabricated. These are test structures with a sensitive area of $5\times5\,\mathrm{mm}^2$ surrounded by a guard ring. Before irradiation, the maximum CCE is achieved at room temperature with voltages above 50–80 V. The diodes were irradiated with neutrons in the TRIGA reactor of Ljubljana. During irradiation the samples were kept at room temperature. The properties of the investigated detectors are summarized in Table 1.

The four samples were irradiated with different fluences in order to check the dependence of the Lazarus effect on the density of radiation induced defects. The minimum fluence value of 10^{14} n/cm^2 exceeds the value for bulk-type inversion [6]. The detectors #1, #2 and #4 were kept at room temperature after irradiation and were heated to reach the annealing state corresponding to about one year of room temperature storage. The sample #3 was stored at -18°C and only after the first series of measurements was heated to reach the same annealing state as the other samples. This procedure allowed a measurement in both the annealed and the non-annealed states, in order to judge how important is the reverse annealing process for the CCE at cryogenic temperatures.

The experiments were performed in a cryostat similar to that described in Ref. [7], consisting of a Dewar vessel and an insert. The insert is a

Table 1
Parameters of the investigated diodes. The resistivity values are those before irradiation

Diode	Fluence (n/cm^2)	Thickness (μm)	Resistivity (kΩ cm)
#1	1×10^{14}	350	1.8
#2	5×10^{14}	400	4.0
#3	1×10^{15}	400	4.0
#4	2×10^{15}	300	2.7

vacuum-tight stainless-steel tube in which the detector, the trigger diode and the radioactive source are mounted. The tube was inserted into a transport Dewar containing liquid nitrogen. The tube walls are in direct contact with the liquid nitrogen around the sample area and are therefore thermalized at 77 K. The sample under investigation is cooled by means of helium exchange gas at 100 mbar pressure. The temperature was monitored using a silicon diode thermometer connected to a copper support structure onto which the detector and trigger printed circuit boards (PCBs) are fixed by screws. The experimental configuration is shown schematically in Fig. 1.

The detectors were exposed from the p^+ side to electrons with a maximum energy of 2.3 MeV from a ^{90}Sr β-source. The selection of Minimum Ionizing Particles (MIPs) was done using a second silicon detector placed behind the detector under study. This trigger detector was read out by means of a fast charge amplifier (AmpTek A225) at room temperature, directly connected via a coaxial cable. The high voltage (HV) was applied to the trigger detector on the n^+ side by means of conductive epoxy. The p^+ side was grounded via a 50 Ω resistor. The guard-ring was connected to ground. The signal from the detector under study was read out from the n^+ side (using a decoupling capacitor) by means of a GaAs FET mounted on the copper support structure. This FET acts as the front-end of a charge amplifier with subsequent stages (AmpTek A250) at room temperature and is operational down to 1 K. The feedback loop includes the long cables from the FET to the amplifier. The noise of this amplifier is about 1500 electrons FWHM. The charge signal was then shaped (with 1 μs shaping time) and sent to a MultiChannel Analyzer (MCA) for recording and producing the collected charge distributions.

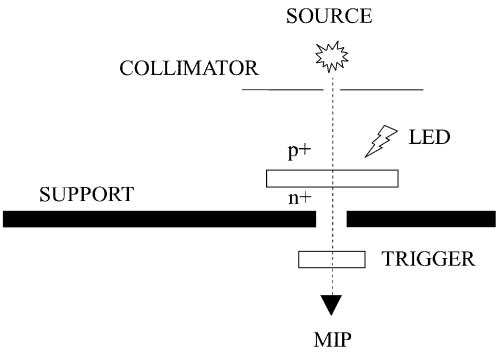

Fig. 1. Schematic illustration of the experimental layout.

The absolute calibration of the charge recorded by the MCA was obtained using two non-irradiated detectors of 300 and 400 μm thicknesses coming from the same wafers as detectors #2, #3 and #4, operated above the full depletion voltage. The stability of the calibration was also checked periodically by means of a test pulse injecting 4 fC to the input of the amplifier via a 0.6 pF capacitor. A typical spectrum obtained with detector #3 (irradiated up to 1×10^{15} n/cm^2) is shown in Figs. 2. The most probable value of the charge collected in the diode was determined by fitting the charge spectrum with a Landau distribution function. The pedestal was fit by a Gaussian function. The CCE was then obtained by subtracting the pedestal from the most probable value, and by normalizing the result using the calibration values from the

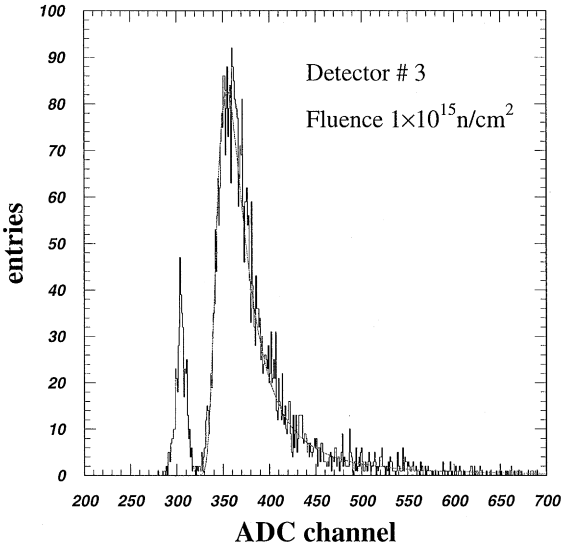

Fig. 2. A typical charge distribution obtained for detector #3 (fluence 10^{15} n/cm^2) at 77 K and 250 V reverse bias. The most probable value of the Landau distribution is 356.6 ± 0.2, and a Gaussian fit to the pedestal gives the mean value of 304.7 ± 0.3, with RMS deviation of 5.4 ± 0.3. The normalized CCE is 20%.

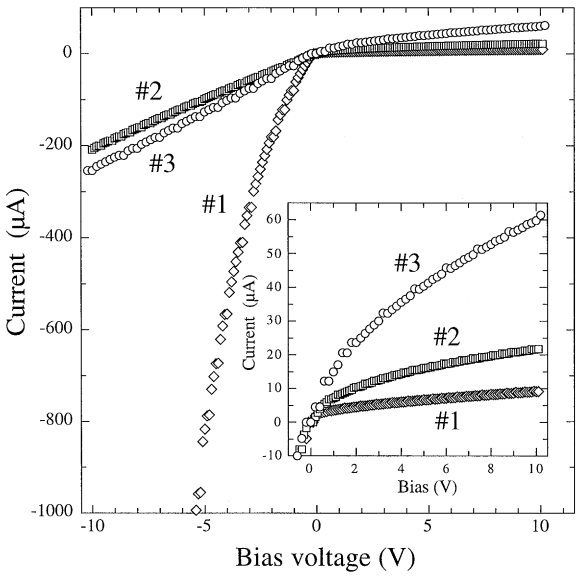

Fig. 3. Current–voltage characteristics measured at 300 K at both bias voltage polarities, for detectors #1, #2 and #3 which were irradiated to fluences given in Table 1. In the insert, reverse current is shown on a blown-up scale.

reference detectors. The statistical error related to the quality of the fits was added linearly to the systematic error due to the uncertainty in the detector thicknesses. These systematical errors are included in the figures.

3. Current–voltage characteristics

In order to measure the current–voltage characteristics (I–V) of the detectors we used a Keithley 697 picoammeter connected to the sample under investigation. For these measurements the samples were cooled to 77 K by direct immersion into a liquid nitrogen bath.

The maximum High Voltage (HV) which could be applied was 250 V, limited by the electric isolation on the sample mount. The sensitivity of the current measurements was limited to about 1 nA due to the leakage in the capacitors used for filtering the HV (needed for the CCE measurements discussed in the following sections). The I–V characteristics of the detectors #1, #2 and #3 were measured at room temperature and 77 K; the room temperature results are plotted in Fig. 3. The detector #4 behaves similarly to detector #3; therefore it is not shown in the figure. The comparison of the I–V curves in Fig. 3 shows a regular increase of the current with fluence at reverse polarization, an observation which is in agreement with the results of the ROSE collaboration [6]. However, the forward current characteristic shows some differences. The detector #1 features an exponential rise of the current, whereas at higher fluences (detectors #2 and #3) the I–V curves are almost linear, close to ohmic characteristics.

At 77 K the reverse leakage currents are all compatible with zero within the resolution limited by the leakage of the capacitors. Under forward bias voltage the currents are also compatible with zero, except for detector #1 which has a breakdown at -30 V. In detectors #2 and #3 the bulk material behaves as a resistor of very high value; this effectively limits the current also in the forward direction of the applied voltage down to -250 V.

4. CCE results for conventional reverse-bias operation

In order to determine the CCE, the following experimental procedure was used. The sample was mounted and the insert was evacuated until the pressure was reduced to 10^{-5} bar. The tube was then immersed into liquid nitrogen. From this moment the sample starts to cool due to thermal radiation and to the small amount of residual gas which create a weak thermal link with the tube wall at 77 K. The bias voltage setting, chosen for the temperature scan, was applied and the leakage current was monitored together with the temperature. As soon as the leakage current was reduced to such a value that the noise was below 2000 electrons FWHM, the measurements of the CCE were started. The temperature changed by less than 1 K during the 20 s interval needed for recording the spectrum from which the CCE was determined.

Once the temperature reached the value of 77 K, the voltage scan was started. For each bias voltage the measurements was preceded by detector conditioning in unbiased state for at least 15 min. This

was done to achieve stable conditions for the filling of the charge carrier traps, as will be discussed in Section 6. The desired bias voltage was then applied, and the corresponding CCE was measured. It is worth mentioning that in materials rich in deep-level traps, the history of the bias voltage plays a crucial role in the time evolution of the amplitude of the signal at cryogenic temperatures. For example, reversing the bias polarity generates a transient condition in the bulk, during which the radiation-induced electrical pulses are gradually reduced in amplitude, and change sign only after a few minutes. This process was originally observed in germanium detectors [8] and was called the "detector polarization". It is therefore important to prepare the detector always into stable conditions before modifying the applied bias voltage.

Keeping the bias voltage constant, the CCE measurement was repeated at various time intervals, in order to determine its time dependence. The last measured value of the temperature scan, obtained after waiting for many hours, was cross-checked by waiting overnight with the bias voltage on. The CCE values were in good agreement they can therefore be considered as the stable value of the CCE.

4.1. Temperature dependence of the CCE

The temperature dependence of the CCE for detectors #1, #2 and #3 (Fig. 4) shows some common features. The detector #4 has a temperature dependence which is very similar to that of detector #3 and is therefore omitted in the figure. The three detectors are biased with a voltage such that at high temperature they are certainly not fully depleted (100 V for detector #1 and 250 V for detectors #2 and #3). All detectors show very low CCE values in the high temperature range. A substantial rise of the CCE starts around 180 K, and the CCE reaches its maximum value at a temperature of around 130 K for all samples. Similar effects have also been observed in Ref. [9]. The recovery of the CCE is likely to be associated with an increase in the thickness of the active depleted layer. The temperature of maximum CCE was found to be universal within the experimental accuracy.

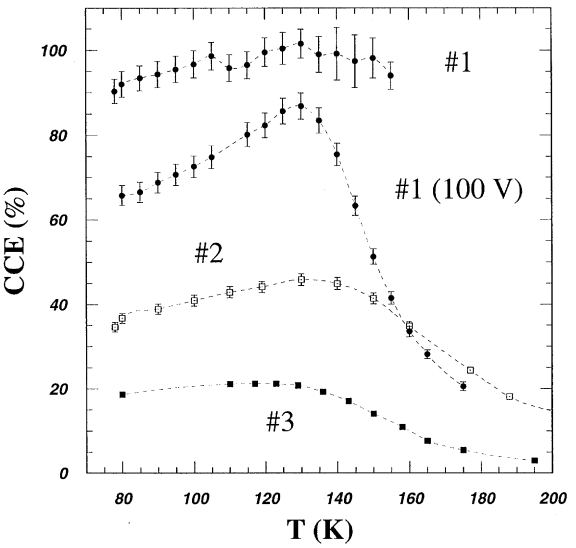

Fig. 4. Temperature dependence of CCE for detectors #1, #2 and #3. The three detectors were measured with a reverse bias voltage of 250 V. The detector #1 was measured also with a reverse bias voltage of 100 V.

The decrease of the CCE observed below 130 K may also be related with a modification in the thickness of the depleted layer, and will be discussed below. The heavily irradiated detectors (#2 and #3) do not reach 100% CCE at the maximum applied bias voltage of 250 V; however, some recovery effect is still observable at low temperatures. A confirmation that the CCE recovery can be related to an increase in the depletion depth is supported by the results of the temperature scan performed for the detector #1 at 250 V. In this case the applied voltage is high enough to fully deplete the device even at intermediate temperatures, and the CCE is close to 100% at all temperatures at which the noise level allowed to perform measurements.

4.2. Voltage dependence

The voltage dependence of the CCE for the three detectors measured at 77 K is shown in Fig. 5. Detector #4 shows results very similar to detector #3 and will be discussed in Section 5 in the context of forward bias operation.

The three detectors show some common features also in this case. The CCE measured immediately after applying the HV sharply increases with the

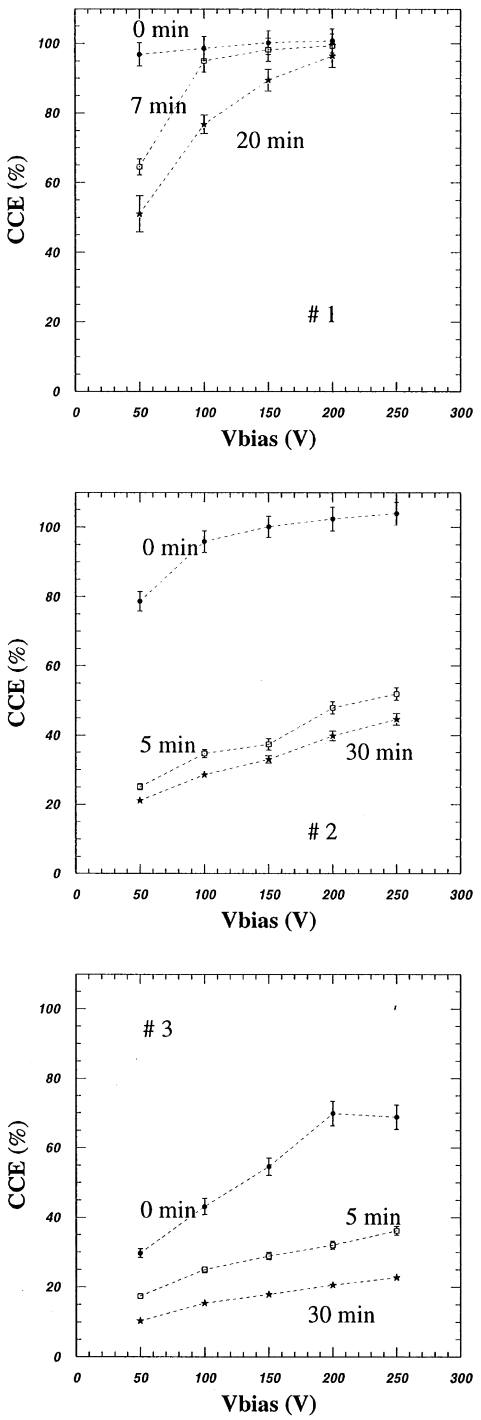

Fig. 5. Voltage dependence of the CCE of detectors #1, #2 and #3 at 77 K, measured at different time intervals after HV turn-on.

applied bias voltage and eventually reaches 100% below 250 V for detectors #1 and #2, while for detector #3 a maximum value of 65% is obtained in 250 V. Another common striking feature is that the CCE decreases with time, i.e. the measurements repeated some time after turn-on of the HV yield a monotonically decreasing CCE, which converges towards a stable value; this will be discussed in the next subsection.

For measurements taken at a given non-zero time after the HV is turned on, the slope of the CCE with the applied bias voltage is smaller. The stable CCE values match the poor results obtained for the CCE in the temperature scans for samples #2 and #3. The maximum CCE obtained for detector #3 immediately after applying the HV, shows a linear increase with the applied voltage up to around 70% at 200 V.

4.3. Time dependence

In order to understand better the time dependence of the CCE, the data of Fig. 5 are plotted in Fig. 6 as a function of time. The lines represent fits to exponential time dependence, and the time constants are given in Table 2. The CCE of detector #1 has a slower decrease with time, the characteristic time being shorter for lower bias voltages. For detectors #2 and #3 the decrease becomes faster and it can be seen that, as a general trend, the larger the applied bias voltage, the higher is the initial CCE value, and the slower it decreases. In these cases, most of the CCE loss takes place in the first 5 min after the HV is applied. It is also important to note that in the case of detector #1 it is possible to completely suppress the time dependence of the CCE by means of a fairly large bias voltage which corresponds to a strong overdepletion. A confirmation that this situation is stable comes from the data of Fig. 4, where the CCE measured at 250 V stays constant at 100% during the temperature scan.

5. CCE results for operation with forward bias voltage and with light

Special experiments were performed with the detectors operating in non-conventional modes. In

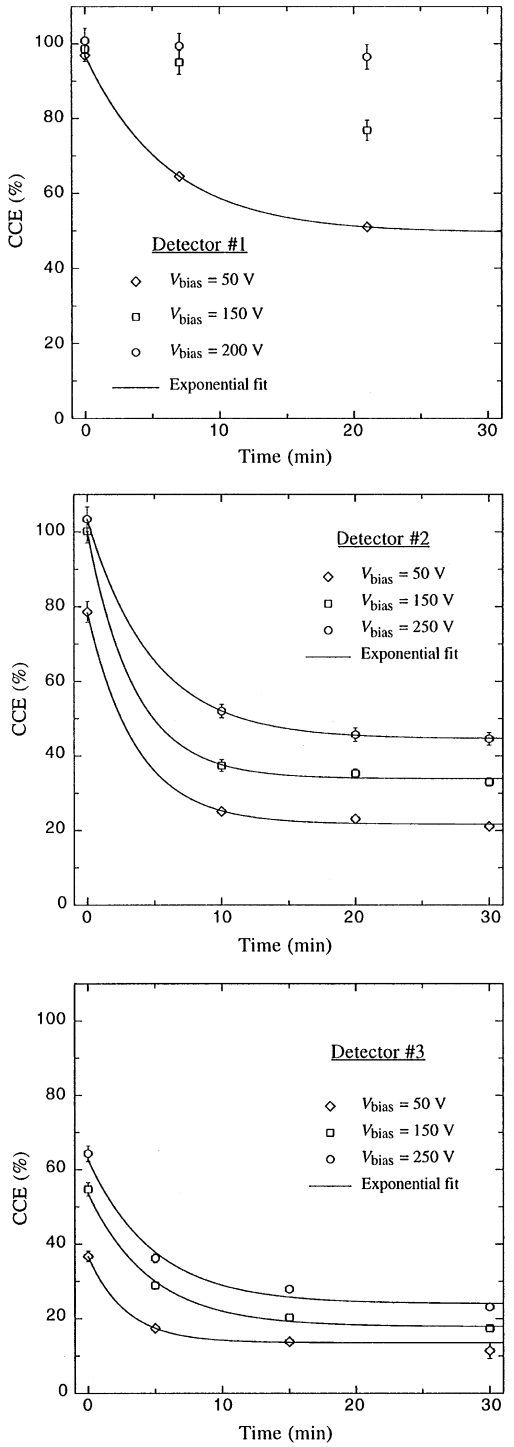

Fig. 6. Time dependence of the CCE at 77 K for detectors #1, #2 and #3, at different reverse bias voltages.

Table 2
Time constants of the CCE exponential decay, obtained from fitting the data of Fig. 6. Only statistical errors are given in this table

Detector	Bias voltage (V)	Time constant (min)
#1	50	6.1 ± 2.0
#2	50	3.6 ± 0.4
#2	150	3.5 ± 0.6
#2	250	4.8 ± 0.8
#3	50	2.9 ± 0.4
#3	150	4.6 ± 0.5
#3	250	4.9 ± 0.6

the first set of such measurements the diodes #2, #3 and #4 were operated under forward bias over an extended voltage range; this was possible due to their symmetric I–V curves, as discussed in Section 3.

The second set of experiments consisted of illuminating the detector using light sources of various wavelengths in order to enhance the steady state current by means of optically generated non-equilibrium carriers. This was done in order to fill the radiation-induced traps and to achieve a better penetration of the electric field in bulk material of the detector, as suggested in Ref. [9].

5.1. Forward bias operation

Forward bias operation has been considered very interesting for heavily irradiated silicon detectors, and promising results have already been obtained in the case of moderate cooling [10]. It is worth stressing, however, that in the case of cryogenic operation, due to very high bulk resistivity, one cannot distinguish this mode from the conventional reverse bias operation, judging from the current passing through the detector.

This mode of operation was possible over an extended bias range only for the detectors #2, #3 and #4; the I–V characteristic of detector #1 shows a large current increase at voltages below -30 V, as was indicated in Section 3.

The temperature dependence of the CCE for detectors #2, #3 and #4 is shown in Fig. 7 for forward bias operation. The CCE starts increasing

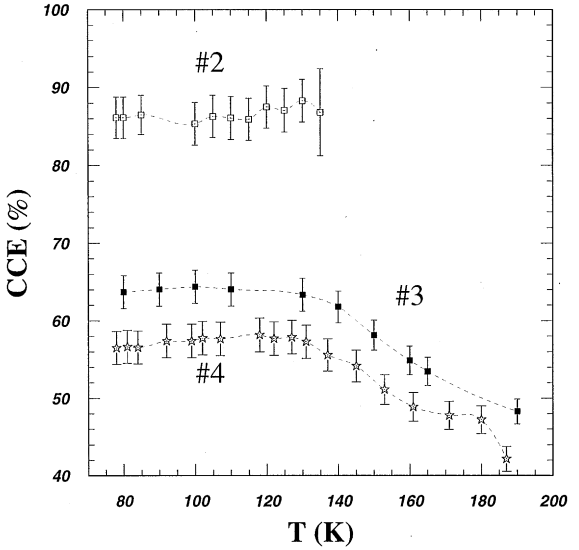

Fig. 7. Temperature dependence of the CCE for detectors #2, #3 and #4. All three detectors were operated at a forward bias voltage of 250 V. Note that the zero of the vertical axis is offset in this plot.

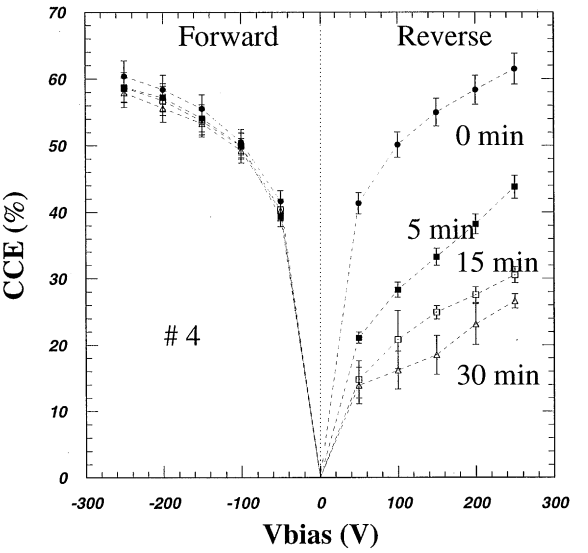

Fig. 8. Voltage dependence of the CCE of detector #4 in the extended voltage range allowed by the forward bias operation. Measurements at different time intervals after HV turn-on are shown.

around 180 K and saturates below 130 K, for all detectors. Measured values are about three times higher than those observed under reverse bias. Moreover, good values of CCE start being recorded as soon as the temperature is low enough to allow performing the measurements. The observation of good CCE values for these relatively high temperatures is in good agreement with previous observations [10,11].

The CCE of detector #4, which was irradiated to the highest fluence, was measured at 77 K over the full range of available bias voltages, the results being shown in Fig. 8. The CCE is about three times higher with forward bias than with reverse bias in stable conditions. Besides, under forward bias operation the detector shows a time-independent CCE. In fact, the large values obtained are similar to those observed under reverse bias immediately after switching on the HV. This also correlates with the good improvement observed above in the case of temperature dependence of the CCE. The maximum value, however, does not reach 100% at 250 V. Similar improvements were observed for detectors #2 and #3.

5.2. Light illumination

In order to illuminate the front side (p^+) of the detector, various LEDs were placed on the detector PCB. The colours of the four light-emitting sources were: near Infra-Red 850 nm (IR), Red (R), Yellow (Y) and Green (G). These LEDs are commercial devices which were checked for their functionality at 77 K by visual inspection of the diode immersed into a liquid nitrogen bath. A precise determination of the wavelength and its possible shift with the temperature was beyond the scope of this work. The intensity of the emitted light could be adjusted by controlling the current in the LED and by observing the corresponding detector bias current. The illumination was maintained on a constant level during the CCE measurements.

The intensity of the applied light was adjusted so that the leakage current was about 5 nA, not adding a significant contribution to the overall noise of our measurement system. The CCE of detector #4 (the one with highest radiation fluence) was measured over the full bias range and is shown in Fig. 9. The main effect of the light

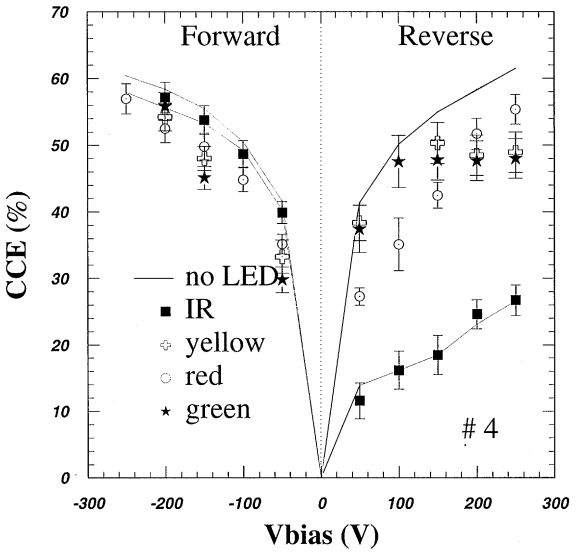

Fig. 9. Effect of light illumination on the voltage dependence of the CCE over the entire allowed voltage range for detector #4.

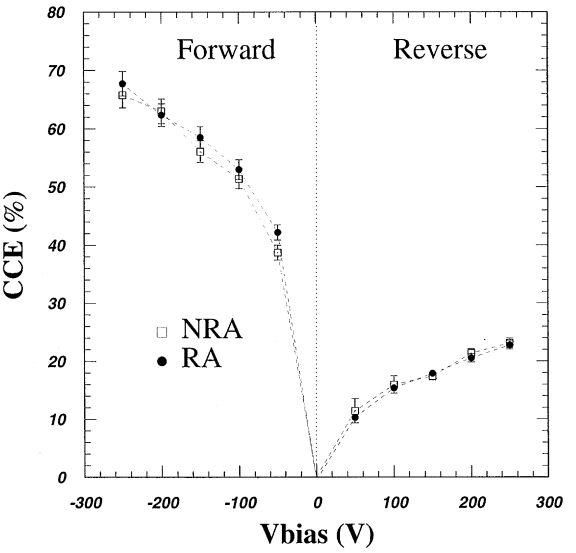

Fig. 10. Effect of reverse annealing on the voltage dependence of the CCE for detector #3. The measurements cover the full allowed voltage range including forward biasing. At reverse bias the stable saturated values are plotted.

illumination is that no time dependence of CCE is observed. The measured CCE, however, depends on the wavelength and on the applied bias polarity.

In the case of reverse bias operation and illumination with short wavelength light (Y, G), the good values of CCE were obtained immediately after switching on the HV and were maintained without temporal decay. The IR light also has the effect of stabilizing the CCE, but yields values on the level of the saturated CCE in the absence of light. Red light produced an intermediate effect. Despite good noise performance in reverse bias operation, the quality of the fits to the Landau distribution was slightly deteriorated, as reflected in the error bars in Fig. 9. This effect could be due to the non-uniformity of the illumination of the sensitive area of the diode.

Under forward bias, the CCE in the presence of light is compatible, within experimental errors, with the CCE without light.

5.3. Annealing effects

The possible effects of the reverse annealing process on the CCE recovery were investigated on sample #3 (fluence 1×10^{15} n/cm^2), as discussed in Section 2. The CCE was measured before and after annealing over the full allowed bias range, as shown in Fig. 10. No significant difference is found between these two sets of measurements. This suggests that the deep defects, which can be deactivated by means of operation at cryogenic temperatures, are formed during (or soon after) irradiation at room temperature, and are not seriously affected by the reverse annealing process.

6. Discussion and conclusions

The experimental results presented in this paper can be summarized as follows:

(1) The CCE of heavily irradiated silicon diodes is recovered at temperatures below 130 K. This temperature corresponds to the maximum achievable CCE for all the detectors studied, and is independent of the irradiation fluence, of the detector structure, and of the polarity of the bias voltage. At temperatures below 130 K, the CCE saturates in the case of forward bias operation, while it slightly decreases under reverse bias.

(2) In the case of reverse bias operation at 77 K, the CCE shows a time evolution after HV turn-on, decreasing from a high value to a reduced saturated value. The time constant depends on the fluence and on the bias voltage, and it is of the order of 3 to 6 minutes. For the most irradiated sample (2×10^{15} n/cm^2), the saturated value at 250 V and 130 K corresponds to a most probable signal of about 5000 electrons from a MIP. However, in forward bias or with light illumination the most probable MIP signal is 15 000 electrons.

(3) Detectors irradiated to a fluence of 5×10^{14} n/cm^2 or higher show a negligible bias current for both polarities of the applied bias voltage when operated at cryogenic temperatures. This allows operation under forward bias voltage. In this case, the CCE show no time dependence for all samples. In fact, the measured CCE values do not differ from those observed in reverse bias mode just after turning the HV on. Similar results can also be obtained by increasing the steady-state current in reverse bias by illumination with short wavelength light. In the case of the sample irradiated with 2×10^{15} n/cm^2, a most probable signal of about 15 000 electrons can be collected using non-conventional operation.

(4) In the case of operation at cryogenic temperatures, no effect of reverse annealing process was observed.

These results can be qualitatively interpreted in the framework of the present understanding of the filling of deep-level radiation-induced traps. These traps play an important role for the CCE at cryogenic temperatures, as was already suggested in Ref. [9].

It is well known [12] that the conductivity of heavily irradiated silicon detectors is related to the deep-level defects, rather than to the shallow-level dopants as in the non-irradiated material. As a result, already at room temperature the non-depleted region of a diode has a resistivity close to that of an insulator, after the material has undergone type inversion. In this case, the non-sensitive layer of the detector acts as a capacitive divider, which reduces the signal collected at the electrodes. The signal measured in a detector of total thickness D is then proportional to Qd/D, were Q is the total charge generated in the active layer of thickness d. In the case of a MIP, where Q is proportional d/D, one expects a charge collection efficiency which behaves as $(d/D)^2$.

The CCE also depends on charge trapping [7,13]. If the electrons and holes generated by ionization are trapped during their drift, some fraction of the signal is lost, and the CCE is less than 100% even for a fully depleted detector. Consequently, the CCE can be qualitatively expressed as

$$\mathrm{CCE} \propto \left(\frac{d}{D}\right)^2 \exp\left(-\frac{t_{\mathrm{drift}}}{\tau_{\mathrm{trap}}}\right) \tag{1}$$

where t_{drift} is the drift time of the excited carriers, and τ_{trap} is the trapping time constant related to the radiation-induced deep levels. The thickness d of the active layer for an under-depleted detector depends on the applied bias voltage V and on the space charge density N_{eff} according to the relation

$$d = \sqrt{\frac{2\varepsilon\varepsilon_0 V}{e|N_{\mathrm{eff}}|}}. \tag{2}$$

All samples of the present study were irradiated beyond space charge sing inversion, and the N_{eff} at room temperature is therefore negative. When the temperature decreases, the emission process is drastically suppressed due to the exponential dependence of the emission time constant τ_{d} on temperature:

$$\frac{1}{\tau_{\mathrm{d}}} \propto \exp\left(-\frac{E_{\mathrm{t}}}{kT}\right) \tag{3}$$

where E_{t} is the trap energy and k the Boltzmann constant. It is worth reminding that this effect is important only for deep traps in the silicon band gap, for which E_{t} is of the order of ~ 0.5 eV, while it is less pronounced for very shallow defects.

The very long emission time, caused by the reduced lattice thermal energy, has in fact a double effect. The trapping/emission process is strongly unbalanced, leading to filling of a significant fraction of deep levels which reduced $|N_{\mathrm{eff}}|$ until it finally reaches a value near zero. This reduction of $|N_{\mathrm{eff}}|$ leads to an increase of d and consequently of the CCE for a given bias voltage below full depletion. Moreover, the filled traps do not capture any more the radiation-induced carriers, thus

contributing an additional beneficial effect in the trapping term. In such a way, improvements in the CCE can be achieved due to both factors in Eq. (1).

The trap-filling process seems to reach a maximum effectiveness at a temperature of about 130 K, while the CCE decreases at lower temperatures for all detectors. Similar results have been obtained with the technique of laser-filling, discussed in Ref. [9]. The decrease below 130 K might be explained by a possible overcompensation, which brings N_{eff} to a positive value. It is interesting to note that, in the case of detector #1 measured at 250 V, no temperature dependence of the CCE was found. Again, this is in good agreement with the previous discussion, assuming that 250 V corresponds to full depletion, with no trapping losses due to reduced temperature. This interpretation is also compatible with the results obtained with a double-sided microstrip detector irradiated to a fluence similar to that of sample #1 [5].

The time dependence of the CCE at 77 K, shown in Figs. 5 and 6, is a most striking phenomenon. The procedure described in Section 4 allowed to perform each measurement with the same initial filling status of the deep traps, and eliminated by accumulated charge in the detector bulk, possibly remaining from the previous measurement. The CCE degradation rate is a function of the fluence and of the (reverse) bias voltage applied to the detector. In the case of detector #1 (Fig. 6), the CCE degradation takes place in less than 10 min at 50 V, while at 150 V the decrease of CCE starts after a delay $t_{\mathrm{d}} \sim 4$–6 min. At the bias voltage of 200 V, the decrease is less important, the saturated CCE value being $\sim 90\%$, and the delay time is longer, approximately $t_{\mathrm{d}} \sim 15$–20 min. For higher fluences (detectors #2 and #3) the CCE degradation takes place in the first 5 min, and its absolute value does not depend on the applied bias voltage. Moreover, the initial value does not reach 100%. The data seem to indicate that just after HV turn-on, the detector behaves as if it were fully depleted. The CCE degradation could be related with the change in time of N_{eff} and consequently of the geometrical factor due to the d/D ratio. The quantitative explanation of the data, however, requires accurate knowledge of the leakage currents and of deep trap concentrations for each detector. The determination of these was beyond the scope of the present study.

Silicon detectors, irradiated to fluences $> 10^{14}$ n/cm^2, can be operated under forward bias, because of the high resistivity of the bulk at 77 K. Forward biased detectors can be considered as resistors rather than depleted diodes. The CCE values, obtained in such a mode of operation, coincide with those reached in reverse bias mode just after HV turn-on. The CCE as a function of temperature under forward bias increases when the temperature decreases to 130 K, and then stays constant.

We have also shown (Fig. 9) that it is possible to stabilize the CCE at the maximum value obtained soon after applying the HV, by operating the detectors at 77 K in presence of light. In this way it is possible to increase and adjust the steady state current flowing through the detector bulk. It is important to note the striking differences between the IR and the visible light, presumably related with the difference in the absorption lengths, leading to injection of both types of carriers (IR light) or only electrons (visible light) in the detector bulk. The beneficial effect, observed in the case of the visible light, could again be related to reduction of $|N_{\mathrm{eff}}|$ due to additional filling of the traps. These results are compatible with those obtained with microstrip detectors, in the case of current injected in the detector bulk [5].

Finally, in order to compare the investigated devices having different thicknesses, the collected charge per micron of thickness is plotted in Fig. 11 as a function of the applied electric field, in the case of forward bias mode. As was already mentioned, similar results can be obtained under reverse bias if a suitable technique, such as light illumination, is applied in order to stabilize the CCE at its maximum value.

The results presented in this paper demonstrate that silicon detectors, irradiated to high doses, restore most of their operating performance when cooled to cryogenic temperatures. At 77 K it has been observed that the CCE value for the most heavily irradiated detector (2×10^{15} n/cm^2) reaches 60%, corresponding to a most probable MIP signal of 15 000 electrons. This remarkable result relies on bias voltages below 250 V. Moreover, operation

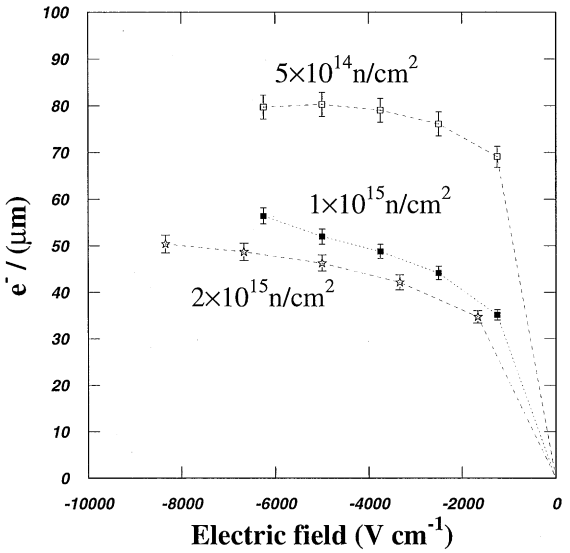

Fig. 11. Applied average electric field dependence of the charge collected per unit thickness at 77 K, for detectors #2–4 in forward bias mode.

at cryogenic temperatures eliminates the leakage current and permits forward bias operation. The Lazarus effect thus leads to higher radiation hardness, obtained by cooling standard silicon detectors with liquid nitrogen. A systematic study of the properties of silicon at cryogenic temperatures under different experimental conditions is currently in progress.

Acknowledgements

We are grateful to Prof. Klaus Pretzl for his interest and continuous support of this work.

This research was supported by the Schweizer Nationalfonds zur Förderung der wissenschaftlichen Forschung (FORCE), by the Stiftung zur Förderung der wissenschaftlichen Forschung an der Universität Bern, and by the Ministry of Science and Technology of the Republic of Slovenia. One of the authors (L.C.) acknowledges financial support from the EC (TMR programme) under contract number ERBFMBICT961204. Three authors (S.R.H.D., C. da V. and V.G.) acknowledge financial support from the Particle Physics and Astronomy Research Council (PPARC). One of the authors (S.R.H.D.) is grateful to Rutherford Appleton Laboratory for his CASE award. The work of two of the authors (B.D. and Z.L.) was supported by the U.S. Department of Energy, Contract Number DE-AC02-98CH10886.

References

[1] V. Palmieri et al., Nucl. Instr. and Meth. A 413 (1998) 475.
[2] RD39 Collaboration, K. Borer et al., CERN/LHCC 98-27, DRDC P53 Add. 1 (1998).
[3] D. Zontar, V. Cindro, G. Kramberger, M. Mikuz, Nucl. Instr. and Meth. A 426 (1996) 51.
[4] M. Moll, E. Fretwurst, G. Lindström, Nucl. Instr. and Meth. A 426 (1999) 87.
[5] K. Borer et al., Nucl. Instr. and Meth. A 440 (2000) 17.
[6] RD48 Collaboration. V. Augelli et al., CERN/LHCC 98-39, LEB Status Report/RD48 (1998).
[7] V.G. Palmieri et al., Nucl. Instr. and Meth. A 417 (1998) 111.
[8] V. Eremin et al., Sov. Phys. Tech. Semicond. 8 (1974) 1157.
[9] B. Dezillie, V. Eremin, Z. Li, IEEE Trans. Nucl. Sci. 46 (1998) 221.
[10] L.J. Beattie et al., in proc. Elmau Workshop "New developments on radiation detectors", 8th European Symposium on Semiconductor Detectors, Schloß Elmau, June 14–17, 1998, in press.
[11] A. Chilingarov, T. Sloan, Nucl. Instr. and Meth. A 399 (1997) 35.
[12] Z. Li, H.W. Kraner, IEEE Trans. Nucl. Sci. NS-38 (1991) 244.
[13] L. Beattie et al., Nucl. Instr. and Meth. A 412 (1998) 238.